IMAGE PROCESSING TECHNIQUES FOR IMPROVED POROSITY ESTIMATION

Nader Saffari and Amit Som
Dept. of Mechanical Eng.
University College London
London WC1E 7JE, UK

David T. Green
Royal Ordnance plc
Westcott
Aylesbury HP18 0NZ, UK

INTRODUCTION

The work reported here is on the first phase of the development of an automated image analysis package. It is intended that the initial application should be to the problem of porosity estimation in powder metals. Although a great deal of work has been concentrated recently on using ultrasonic velocity changes and attenuation for porosity estimation, the problem can also be addressed through acoustical imaging.

After a C-scan image has been obtained over a certain area of the object, and at a given depth, a visual count of the porosity content is carried out. This operation will eventually be performed by the software being developed.

The objective of this first phase of the work is to obtain a well- resolved binary image of the defect contours. This is so because in the next stage of the process, bright contours on a dark background are detected and tracked. This information is then used for defect classification, which in the simplest case of porosity only present, involves producing a total porosity area and average diameter information.

To this end, several image processing techniques have been investigated. These include four edge-detection methods and a 2-D pseudo-Wiener filter for resolution enhancement.

THE RAW IMAGE

The test object is a piece of epoxy material with six closely spaced surface indentations. The two smaller indentations have a diameter of approximately 150 μm and the larger indentations are 250 μm in diameter. A 64x64 pixel surface image is produced over a 4mm square area (ie pixel size is 62.5 μm square) using a 40 MHz probe with a 3dB focal spot size of approximately 300 μm. This is shown as figure 1.

RESOLUTION ENHANCEMENT

A commonly used technique for the removal of blur and resolution enhancement in acoustical imaging is Wiener inverse filtering [1]. The blur or image unsharpness is due to the practical limitations of the imaging system and sometimes in subsurface imaging it is due to defocussing.

Review of Progress in Quantitative Nondestructive Evaluation, Vol. 12
Edited by D.O. Thompson and D.E. Chimenti, Plenum Press, New York, 1993

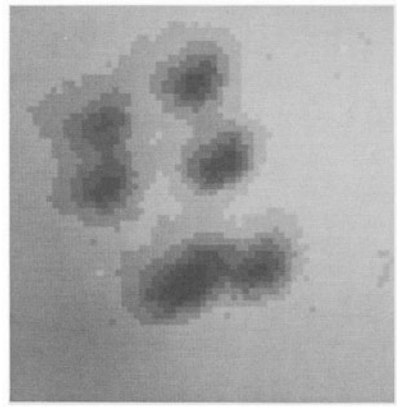

Fig. 1. Unprocessed image of six surface indentations.

Implementation of the parametric Wiener filter in the spatial frequency domain requires a knowledge of the power spectra of the noise and the ideal image. Since this is not readily available we have used a pseudo-Wiener filter of the form:

$$\hat{F}(u,v) = \left[\frac{H^*(u,v)}{|H(u,v)|^2 + K}\right] G(u,v) \qquad (1)$$

where $\hat{F}$ and G are the 2-D Fourier transforms of the restored and the observed image respectively, and H is the transform of the system point-spread function (PSF) which describes the lateral loss of resolution caused mainly by the transducer beam spread. The value of the constant K is empirically determined and typically has a value of $0.001G_{max}$ to $0.005G_{max}$

The PSF is either experimentally obtained by using the image of a single, small pore or a theoretical approximation is used in the form of a 2-D Gaussian described by:

$$h(x,y) = A\exp\left[-\frac{(x-\bar{x})^2}{\sigma}\right] \qquad (2)$$

Two important practical points were noted during implementation of the Wiener filter. The first is that a satisfactory result in terms of signal-to-noise ratio performance is obtained only if the image is low-pass filtered both before and after Wiener filtering. In other words the correct sequence of operations was as follows:

g(x,y) → 2-D FFT → low-pass filter → Wiener filter → low-pass filter → inverse 2-D FFT = f(x,y)

The low-pass filter used was a frequency domain Butterworth filter of order n=3. This LP filtering operation is necessary for the removal of processing noise.

The second observation is that there are differences between the restored images for the actual and the Gaussian PSF's. It can be seen that due to the skewness of the actual PSF compared with the Gaussian, major artifacts are introduced in the restored image with the idealised Gaussian PSF. The difference between the two filtered images, with the corresponding PSF's can be seen in figures 2 and 3.

EDGE-DETECTION

The relative merits of four edge-detection methods were investigated by applying them to the Wiener-filtered image of figure 2(a). These methods were : 1) the Sobel gradient filter; 2) the Marr-Hildreth filter; 3) low-pass transformation and 4) thresholding and Roberts filter.

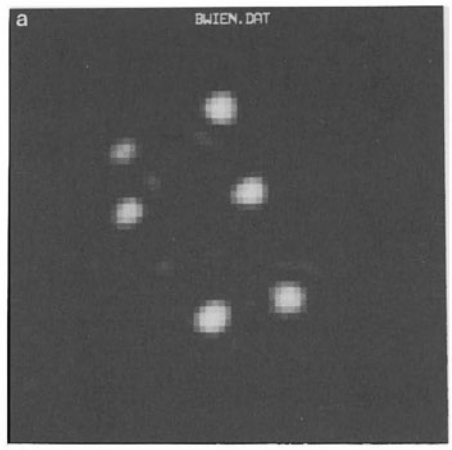

Fig. 2. (a) Wiener filtered image produced with actual PSF as shown in (b).

Fig. 3. (a) Wiener filter with idealised Gaussian PSF as shown in (b).

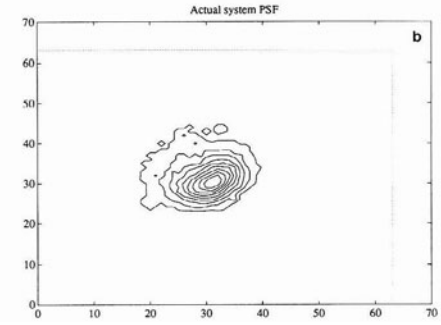

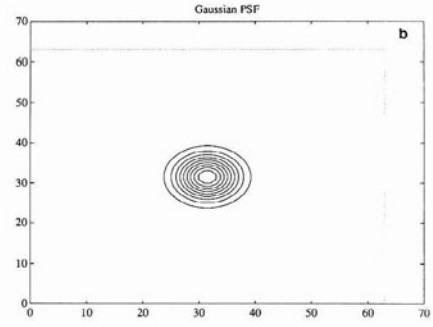

The Sobel Gradient Operator

Edge enhancement by the Sobel operator uses the numerical approximation of a spatial first derivative of the pixel amplitudes [2]. The amplitude of the central pixel within a 3x3 mask is replaced by the sum of the first difference approximations of the partial derivatives $\delta f/\delta x$ and $\delta f/\delta y$. The gradient vectors in the x and y directions are given as:

$$G_x = [f(x+1,y-1)+2f(x+1,y)+f(x+1,y+1)] - [f(x-1,y-1)+2f(x-1,y)+f(x-1,y+1)]$$

$$G_y = [f(x-1,y+1)+2f(x,y+1)+f(x+1,y+1)] - [f(x-1,y-1)+2f(x,y-1)+f(x+1,y-1)] \quad (3)$$

and the resulting overall Sobel gradient operator is then:

$$G[f(x,y)] = [G_x^2+G_y^2]^{1/2} \quad (4)$$

The result of applying this operator to the resolution enhanced image in figure 2(a) is shown as figure 4 below.

The Marr-Hildreth Operator

The Marr-Hildreth method for locating edges is a band-pass filter which should be an optimal tradeoff between high spatial frequency emphasis needed for edge enhancement and low-pass filtering needed for suppression of high frequency noise [3]. The operator is generated by taking the Laplacian of a 2-D Gaussian. This is given as:

$$M(x,y) = A[2(\frac{x-\bar{x}}{\sigma^2})^2 - \frac{2}{\sigma^2}]\exp[-(\frac{x-\bar{x}}{\sigma})^2] \quad (5)$$

where $\bar{x}$ is the mean value and σ is the standard deviation, with A a constant. The choice of σ depends on a tradeoff between low noise and sharpness of image. The filter is implemented as a spatial convolution of the operator with the image, using a 5x5 moving window. A similar tradeoff between low noise and image sharpness determines the size of the moving window (larger window - less noise and more blur). This operator produces the image shown as figure 5.

Low-pass Transformation

This is a method where the result of a Butterworth lowpass filter operation is subtracted from the original image, thereby transforming the image into a high spatial frequency image where the edges are enhanced. Figure 6 shows the result of this filtering operation.

Thresholding and Roberts Edge Detector

A very simple and fast edge detection technique is performed by first creating a binary image through setting an image threshold. The binarization threshold is computed from the grey-level histogram. The histograms investigated here are generally bimodal with two distinct peaks corresponding to the background and the defects. The threshold is set at the dip between the two peaks. For the image in fig. 2(a), this histogram thresholding operation is shown in fig. 8. In applications where the image contains individual defects, location of this threshold will be more difficult.

Next a Roberts gradient filter is applied to the binary image. This is 2-dimensional spatial convolution implemented by a subtraction of the original image from two versions shifted one pixel diagonally in opposite directions, ie:

$$G[f(x,y)] = |f(x,y)-f(x+1,y+1)| + |f(x+1,y)-f(x,y+1)| \quad (6)$$

The result is a one pixel wide closed contour generated from the binary image, as shown in figure 7. It can be seen that this operation, which is in fact the simplest and fastest method investigated, does produce the best result.

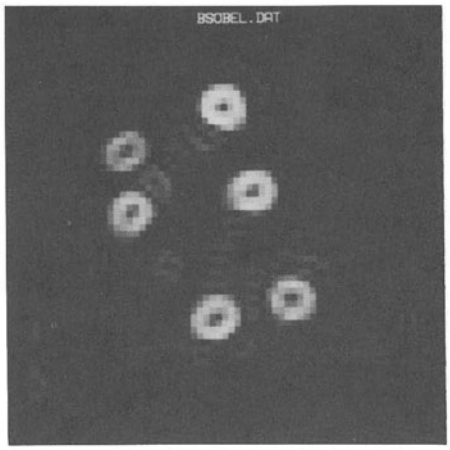

Fig. 4. Sobel gradient filter applied to the Wiener filtered image in fig. 2(a).

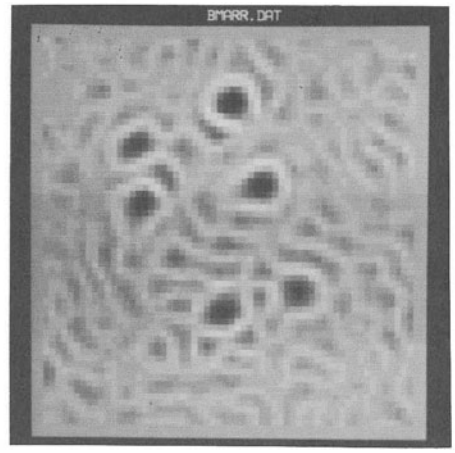

Fig. 5. Marr-Hildreth filter applied to the image in fig. 2(a).

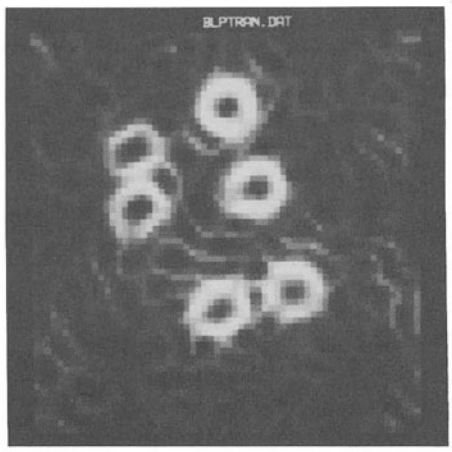

Fig. 6. Low-pass transformation applied the image in fig. 2(a).

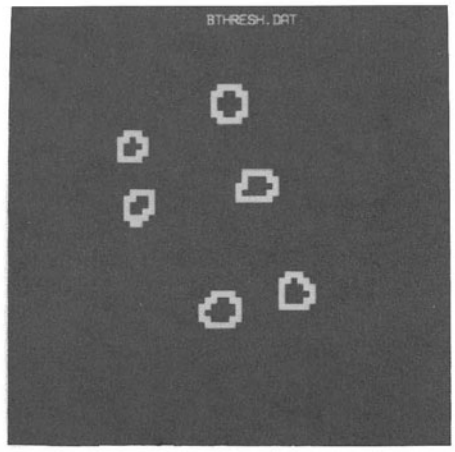

Fig. 7. Thresholding plus Roberts filter applied the image in fig. 2(a). The result is the binary image of the defect contours.

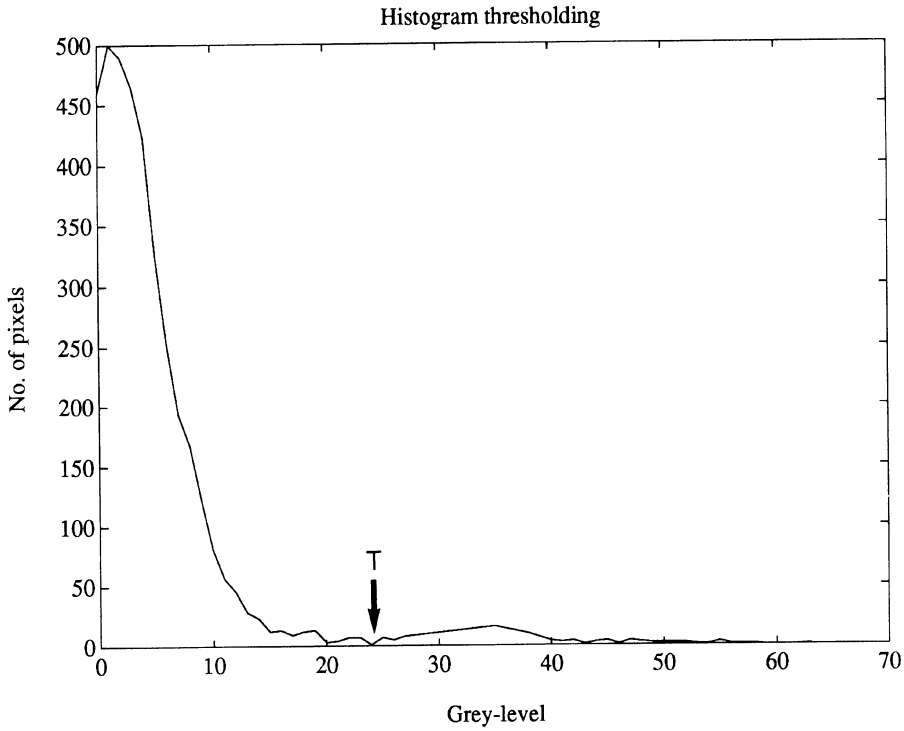

Fig. 8. Histogram of the image in fig. 2(a), used for obtaining the binarization threshold in fig. 7.

CONCLUSIONS

We have investigated the use of pseudo-Wiener filtering followed by several edge-detection techniques for the removal of blur and sharpening of the edges in images of simulated porosity. It can be seen that a combination of pseudo-Wiener filtering followed by thresholding and Roberts filtering produces an image which is close to the ideal binary image of the defect contours. The simplicity of the operations involved in producing the binary image suggests that real-time implementation could be possible. It is planned for the technique chosen above to be incorporated into an automated defect classification algorithm.

REFERENCES

1. Mitchell KW and Gilmore RS (1992) , in 'Review of Progress in Quantitative NDE', eds Thompson DO and Chimenti DE, vol 11A, Plenum Press, pp 895-902.

2. Gonzalez RC and Wintz P (1987), 'Digital Image Processing', Addison-Wesley.

3. Frock BG and Karpur P (1989), in 'Review of Progress in Quantitative NDE', eds Thompson DO and Chimenti DE, vol 8A, pp 701-708.